THE ASTRONOMICAL JOURNAL, 121:1413–1424, 2001 March

VLA H I LINE OBSERVATIONS OF THE EXTREMELY METAL-POOR BLUE COMPACT DWARF GALAXY SBS 0335−052

SIMON A. PUSTILNIK
Special Astrophysical Observatory, Russian Academy of Sciences, Nizhnij Arkhyz, Karachai-Circassia 369167, Russia; and Isaac Newton Institute of Chile, SAO Branch, Nizhnij Arkhyz, 369167, Russia; sap@sao.ru

ELIAS BRINKS
Departamento de Astronomía, Universidad de Guanajuato, Apdo. Postal 144, Guanajuato, 36000, Mexico; ebrinks@astro.ugto.mx

TRINH X. THUAN
Department of Astronomy, University of Virginia, P.O. Box 3818, Charlottesville VA 22903; txt@starburst.astro.virginia.edu

VALENTIN A. LIPOVETSKY[1]
Special Astrophysical Observatory, Russian Academy of Sciences, Nizhnij Arkhyz, Karachai-Circassia 369167, Russia

AND

YURI I. IZOTOV
Main Astronomical Observatory, National Academy of Sciences of Ukraine, 03680, Kyiv, Ukraine; izotov@mao.kiev.ua
Received 2000 March 1; accepted 2000 November 14

ABSTRACT

We present the results of H I mapping with the NRAO[2] VLA of one of the most metal-deficient blue compact dwarf (BCD) galaxies known, SBS 0335−052, with an oxygen abundance only 1/40 that of the Sun. We study the structure and dynamics of the neutral gas in this chemically young object with a spatial resolution of 20″.5 × 15″ (∼5.4 × 3.9 kpc at an assumed distance of 54.3 Mpc), a sensitivity at the 2 σ detection level of ∼2.0 K or 7.5×10^{19} cm^{-2} and a velocity resolution of 21.2 km s^{-1}. We detected a large H I complex associated with this object having an overall size of about 66 by 22 kpc and elongated in the east-west direction. There are two prominent, slightly resolved peaks visible in the integrated H I map, separated in the east-west direction by 22 kpc (84″). The eastern peak is nearly coincident with the position of the optical galaxy SBS 0335−052. The western peak is about a factor of 1.3 brighter in the H I line and is identified with a faint blue compact dwarf galaxy, SBS 0335−052W, with $m_B = 19.4$, and a metallicity close to the lowest values known for BCDs, about 1/50 that of the Sun. The radial velocities of both systems are similar, suggesting that the two BCDs, SBS 0335−052 and SBS 0335−052W, constitute a pair of dwarf galaxies embedded in a common H I envelope. Alternatively, the BCDs may be the nuclei of two distinct interacting primordial H I clouds. The estimated total dynamical mass, assuming the BCDs form a bound system, is larger than $\sim 6 \times 10^9\ M_\odot$, compared with a total gaseous mass $M_{\rm gas} = 2.1 \times 10^9\ M_\odot$ and a total stellar mass $M_{\rm star} \leq 10^8\ M_\odot$. Hence, the mass of the SBS 0335–052 system is dominated by dark matter. Because of the disturbed H I velocity field and the presence of what might be tidal tails at either end of the system, we favor the hypothesis of tidal triggering of the star formation in this system. It can be due to either the nearby giant galaxy NGC 1376 or the mutual gravitational interaction of the two H I clouds.

Key words: galaxies: compact — galaxies: evolution — galaxies: individual (SBS 0335−052) — galaxies: ISM — galaxies: kinematics and dynamics — ISM: H I

1. INTRODUCTION

Galaxy formation remains a key issue in observational cosmology. While much progress has been made in finding large populations of galaxies at high ($z > 3$) redshifts (e.g., Steidel et al. 1996; Dey et al. 1998), truly young galaxies in the process of forming, defined as objects that are experiencing their first epoch of star formation, remain elusive. The spectra of those distant galaxies generally indicate the presence of a substantial amount of heavy elements, implying previous star formation and metal enrichment.

We adopt here a different approach for studying truly young galaxies. Instead of searching for high-redshift objects, we look for nearby young dwarf galaxies that are possibly undergoing their first burst of star formation. As pointed out more than a quarter of a century ago by Sargent & Searle (1970) and Searle & Sargent (1972), some low-mass galaxies in the local universe may approximate galaxies in an early stage of their formation. Later, Thuan & Martin (1981) identified blue compact dwarf (BCD) galaxies as a class of low-luminosity ($M_B \gtrsim -18$) extragalactic systems undergoing a strong burst of star formation (SF) while exhibiting extremely low heavy-element abundances.

For many years the best candidate for a truly young galaxy has been I Zw 18 ≡ Mkn 116, with a metallicity, Z, of about 1/50 $Z_\odot$ (e.g., Lequeux et al. 1979). Studies of this galaxy in the last decade suggest indeed that it is chemically unevolved. Its extremely low metallicity, derived from the H II region–like spectrum, has been confirmed by many subsequent studies (see Izotov & Thuan 1998 and references therein). Observations in neutral hydrogen (H I) show that it is a very gas-rich system (Lequeux & Viallefond 1980; Viallefond, Lequeux, & Comte 1987; van Zee et al. 1998b). Also,

[1] Deceased 1996 September 22.

[2] The National Radio Astronomy Observatory (NRAO) is operated by Associated Universities, Inc., under contract with the National Science Foundation.

its H I gas appears to have an extremely low metallicity (Kunth et al. 1994), although this last point is considered controversial (Pettini & Lipman 1995; van Zee et al. 1998b).

Until the end of the 1980s, I Zw 18 remained the only BCD with a heavy-element abundance as low as $Z_\odot/50$. Despite efforts by many investigators to search for BCDs with equally low or lower metallicities, there remained a significant gap in metallicity between I Zw 18 and all other known BCDs. This gap was partially filled when Izotov et al. (1990), using the Russian 6 m telescope, tentatively determined the BCD SBS 0335−052 to have a metallicity lower than that of I Zw 18. However, later Melnick, Heydari-Malayeri, & Leisy (1992) concluded that $Z = 1/41\ Z_\odot$ in SBS 0335−052, making it the second-most metal-deficient galaxy known in the universe. This BCD is now considered one of the best candidates for a galaxy in formation.

A dwarf galaxy experiencing its first burst of star formation should have an extremely low metallicity in its H II regions. Such a galaxy should not show any sign of an older stellar population produced in previous SF episodes. The gas mass would be expected to exceed significantly that in stars. Studies of SBS 0335−052 over the last few years show that it appears to fulfill all those conditions and that it is very probably a truly young galaxy. We briefly summarize its main observational properties.

1. The oxygen abundance in the brightest H II region in the galaxy is found to be $12 + \log (\mathrm{O/H}) = 7.30 \pm 0.01$ (with variations from 7.15 to 7.33 on small scales), only slightly higher than that in I Zw 18 (Melnick et al. 1992; Izotov et al. 1997; Izotov et al. 1999).

2. Blue underlying, extended low-intensity emission is detected in SBS 0335−052 on V- , R- , and I-band images. The blue $V-I$ and $R-I$ color distributions suggest that a significant contribution to the emission of the extended low-intensity envelope is due to ionized gas. It is found that the observed equivalent width of Hβ emission in the extended envelope is 2–3 times weaker than the value expected in the case of pure gaseous emission. This could be explained by the presence of underlying stellar emission from coeval A stars (Izotov et al. 1997; Thuan, Izotov, & Lipovetsky 1997).

3. From the optical colors of the low surface brightness component, together with evolutionary synthesis models, Papaderos et al. (1998) conclude that the age of the underlying stellar population is less than $\sim$100 Myr, with a total mass of $\sim 10^7\ M_\odot$, comparable to the total mass of young blue stars (Izotov et al. 1997). Near-infrared (NIR) colors after correction for the gas contribution are consistent with a stellar population not older than 4 Myr, and the possible contribution to the NIR light from an evolved stellar population in SBS 0335−052 cannot exceed $\sim$15% (Vanzi et al. 2000).

4. No evidence for strong, narrow Lyα emission is found in a UV spectrum obtained with the *Hubble Space Telescope* (*HST*) (Thuan & Izotov 1997). Instead, a damped Lyα absorption line is observed, which implies an H I column density $N(\mathrm{H\ I}) = 7 \times 10^{21}\ \mathrm{cm}^{-2}$, the largest observed so far for a BCD and comparable to the highest column densities observed in Lyα clouds in the direction of quasars. The resonant O I 1302 Å line is also detected. Assuming that the O I line is unsaturated and that it originates in the neutral gas leads to an oxygen abundance in the neutral gas of $\sim$1/37,000 of the solar value, or about 1/900 of that in the H II regions around the young super–star clusters. However, a more consistent interpretation of the UV absorption lines of O, Si, and S is that these lines originate not in the H I but in the H II gas. If this interpretation is correct, then the neutral gas in this system can be pristine and not polluted with heavy elements at all (Thuan & Izotov 1997).

5. Thuan, Izotov, & Lipovetsky (1995) and Izotov & Thuan (1999) have also argued, on the basis of the very small dispersion of the C/O and N/O ratios in extremely metal-deficient BCDs with a metallicity less than 1/20 solar, that in those galaxies C and N are made exclusively by massive ($M > 9\ M_\odot$) stars, because intermediate-mass ($3\ M_\odot \leq M \leq 9\ M_\odot$) stars have not had time to evolve and release their nucleosynthesis products. Izotov & Thuan (1999) suggest that BCDs with $Z < Z_\odot/20$ are young, with ages less than $\sim$100 Myr, the main–sequence lifetime of a 9 $M_\odot$ star being $\sim$40 Myr. Chemical abundances thus also suggest that SBS 0335−052, with $Z = Z_\odot/40$, might be a young galaxy.

In view of the unusual properties of this candidate young galaxy we considered it important to measure its neutral gas content and study the H I structure and velocity field. Measurements of the integrated H I flux of this galaxy in the 21 cm line were carried out with the Nançay radio telescope (NRT) in 1993 (Thuan et al. 1999a). From those data the total H I mass was estimated, which indicates that this galaxy is gas-rich ($M_{\mathrm{H\,I}} \sim 10^9\ M_\odot$), with less than 1/10 of its baryonic mass in stars. The H I flux appeared to be high enough to allow higher resolution mapping with the VLA. In this paper we present the results of VLA observations of SBS 0335−052 and discuss the properties of its H I density distribution and velocity field.

The paper is organized as follows. In § 2 we describe the observations and data reduction. In § 3 we derive the H I density distribution and velocity field. In § 4 we examine the gas and dynamical mass of the system, and in § 5 we focus on various aspects related to the star formation in SBS 0335−052. The paper is summarized in § 6.

2. OBSERVATIONS AND DATA REDUCTION

The blue compact dwarf galaxy SBS 0335−052 was observed with the VLA in the 21 cm line of neutral hydrogen on 1994 December 26 for an on-source time of 163 minutes in the C configuration and on 1995 May 13 for an on-source time of 80 minutes in the D configuration. The C configuration, with baselines between 160 and 15000 wavelengths (or 0.03 and 3 km), was used to achieve angular resolution in H I high enough to resolve features comparable in size to the optical size of the galaxy ($\sim$15″). The D configuration, with baselines between 160 and 5000 wavelengths (or 0.03 and 1 km), was used to achieve high surface brightness sensitivity for gas distributed at larger scales (the 2 σ noise level corresponds to $7.5 \times 10^{19}\ \mathrm{cm}^{-2}$) and to search for companion H I clouds, such as those detected near several other BCDs by Taylor, Brinks, & Skillman (1993), Taylor et al. (1995, and 1996a) and Taylor (1997). Table 1 summarizes the observations.

The observations exploited the 4IF correlator mode. In this mode one IF pair was used to take data over a bandwidth of 1.56 MHz with 63 channels, giving a channel width of 24.4 kHz (5.3 km s^{-1}), while the second IF pair was used over a 3.12 MHz bandwidth with 31 channels, each having a width of 97.7 kHz (21.2 km s^{-1}). The higher velocity

TABLE 1

OBSERVATIONAL PARAMETERS

Parameter	Value 1994 Dec 26	Value 1995 May 13
VLA configuration	C	D
Antennas	26	26
Time on source (minutes)	163	80
Central velocity (km s^{-1})	4043	4043
Half-power beam	20.″5 × 15″	61″ × 45″
Brightness temperature (K) corresponding to 1 mJy beam^{-1}	2.0	0.22
Total bandwidth (MHz)	3.12	3.12
Total channels	31	31
Channel width (km s^{-1})	21.2	21.2
Noise in channel maps (mJy beam^{-1})	0.5	1.0
Total bandwidth (MHz)	1.56	1.56
Total channels	63	63
Channel width (km s^{-1})	5.3	5.3
Noise in channel maps (mJy beam^{-1})	1.0	2.0

resolution data provide detailed information on the galaxy, whereas the lower velocity resolution data cover a larger range in velocity space at higher signal-to-noise ratio (S/N).

The data were edited and calibrated with the NRAO Astronomical Image Processing System (AIPS) package. The C and D configuration observations were calibrated separately and inspected. Once satisfied with the result, the data were combined and Fourier transformed. In the end, data cubes were obtained measuring 512 × 512 pixels, each pixel measuring 5″ on a side. The resulting synthesized beam was 20.″5 × 15.″0. The noise in the final cube, at velocity resolution 21.2 km s^{-1}, is ∼0.5 mJy beam^{-1} in a single channel.

3. H I DISTRIBUTION AND VELOCITY FIELD

In Figures 1 and 2 we show the individual channel maps over the velocity range for which significant signal is detected. The size of the synthesized beam is indicated by the ellipse in the lower left corner of the first channel map in each figure. Figure 1 displays the H I emission associated with SBS 0335−052, which is traced in the channels corresponding to a range in velocity from 4000 to 4085 km s^{-1}. Despite the low signal-to-noise ratio in the channel maps, one can appreciate the rather complex kinematics of the gas. There is an underlying rotation, with the eastern edge of the H I complex receding. A prominent feature in the data cube is a large, almost face-on spiral galaxy, NGC 1376. The channel maps corresponding to the velocities covered by this object are presented in Figure 2. Its velocity ranges from 4064 to 4234 km s^{-1}. The central radial velocity, 4162 km s^{-1} (Rix & Zaritzky 1995), is about 120 km s^{-1} higher than that of our target galaxy.

By adopting a Hubble constant $H_0 = 75$ km s^{-1} Mpc^{-1}, the redshift distance is 54.3 Mpc (Thuan et al. 1997), so that 1″ corresponds to 263 pc. If NGC 1376 lies at the same distance as SBS 0335−052, their projected distance of about 9.′5 then corresponds to 150 kpc.

Figure 3 is a gray-scale presentation of the integrated intensity of the H I in the target field. It is obtained by creating a zeroth-moment map of a blanked data cube, i.e., a data cube in which all signal below the 2 σ level was deleted and in which only those regions are preserved that show emission in at least two successive channels. Both SBS 0335−052 and NGC 1376 are displayed. Notice the elongated structure of the SBS 0335−052 H I cloud with two prominent concentrations separated by about 84″ (or 22 kpc). These peaks are marked "E" and "W," respectively, on the map. They are slightly resolved, as indicated by Gaussian fitting of the brightness distribution of small regions centered on these peaks, and are situated approximately symmetrically relative to the cloud center. The western peak is about a factor of 1.3 brighter than its eastern counterpart. The H I cloud as a whole is quite inhomogeneous.

The east and west H I peaks are embedded in a common elongated envelope with a strong bend at the eastern edge. The outermost contour in Figure 3 corresponds to an H I column density 3×10^{20} cm^{-2} and a size about 31 × 7 kpc. At the 2 σ level above the noise (represented by the lightest gray-scale tones in Fig. 3), which corresponds to an H I column density 1.9×10^{20} cm^{-2}, the total extent of the H I emission is ∼ 66 × 22 kpc. Some additional weak H I features may be present in the field around SBS 0335−052, including an extended object to the northeast. However, these detections are tentative at best and should be confirmed with future higher S/N observations. The structure of the H I feature to the northeast of the SBS 0335−052 H I complex at $\delta = -05°09'30''$ is quite unusual. No cases similar to this one were found in studies devoted to a search for H I companions near H II galaxies (Taylor et al. 1993, 1995) or low surface brightness (LSB) dwarf galaxies (Taylor et al. 1996b).

We should like to emphasize that an H I envelope of this size is rare among BCDs and dwarf irregulars. The typical size of H I envelopes around BCDs is usually a few kiloparsecs (see, for example, the discussion in Viallefond & Thuan 1983 and in van Zee, Skillman, & Salzer 1998a). The only known H I envelope of comparable size is that of H I 1225+01 (Chengalur, Giovanelli, & Haynes 1995).

Figure 4 represents the integrated profile of the H I cloud associated with SBS 0335−052. It was calculated by integrating all the flux in the region around SBS 0335−052, as seen in Figure 3. The dashed lines are used to indicate separately the integrated profiles of the eastern and western halves of the H I cloud. Whereas the integrated profile width measured with the VLA is close, within the errors, to that measured with the NRT (Thuan et al. 1999a), the VLA integrated flux, 2.46 ± 0.18 Jy km s^{-1}, is about a factor of 2 higher than that measured with the NRT (1.28 ± 0.22 Jy km

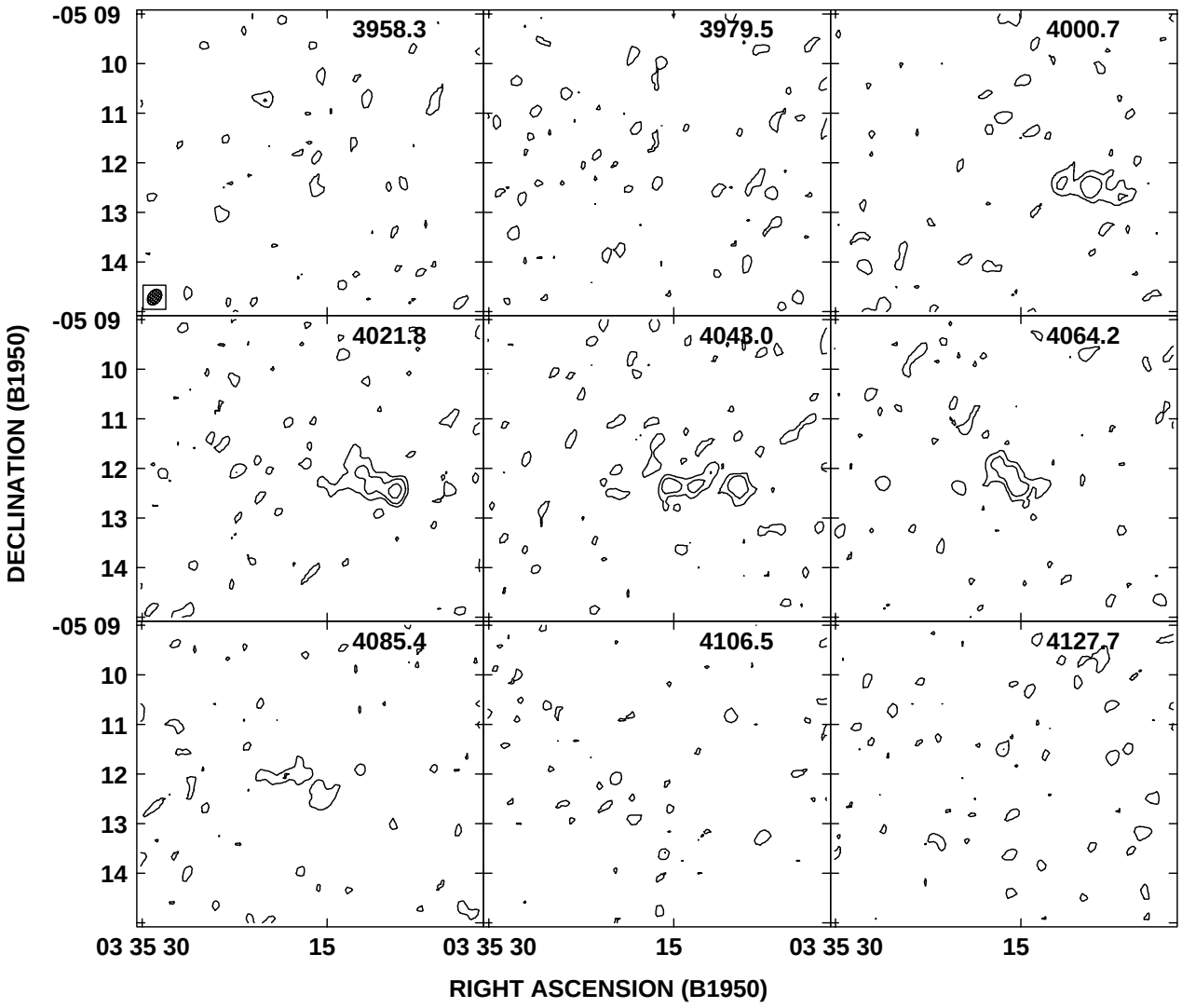

FIG. 1.—Mosaic of channel maps of the low velocity resolution data showing the H I distribution of SBS 0335−052. Contours represent 1 (2 σ), 2, 4, and 6 mJy beam^{-1}. The ellipse in the upper left panel indicates the beam size.

s^{-1}). This difference points to a significant loss of integrated flux for the NRT due to its narrow horizontal beam (FWHM = 3.5) compared with the larger extent of up to $\sim 4'$ of the H I cloud in the east-west direction. After a first-order correction for the NRT beam shape, the NRT/VLA flux ratio becomes 0.78 ± 0.27, which is consistent within the errors.

Figure 5 is an overlay of the H I contours on top of an optical *B*-band image from Papaderos et al. (1998). The optical astrometry was done with six stars, five of which are shown and marked by plus signs in Figure 5. Their coordinates were obtained from the *Hubble Space Telescope* Guide Star Catalog (Lasker et al. 1990) and are listed in Table 2. As shown first by Pustilnik et al. (1997), the two H I peaks are clearly identified with two faint optical galaxies, the eastern one with the object SBS 0335−052 itself and the western peak with a very compact, faint dwarf galaxy with $m_B = 19.4$. A comparison of the optical and H I peak positions will be given in § 4.

No 20 cm continuum emission was detected at the locations of SBS 0335−052 or SBS 0335−052W at the 4 σ level of 1 mJy. To avoid as much confusion as possible, we will use the same nomenclature for the H I components as for the optical counterparts, referring to the eastern H I component simply as SBS 0335−052 and to the western one as SBS 0335−052W. When referring to the entire H I complex we will employ the term "SBS 0335−052 system."

In Figure 6 we show an enlarged image of the integrated H I flux distribution in the SBS 0335−052 system, the gray scale being a linear representation of the integrated H I flux,

TABLE 2

COORDINATES OF REFERENCE STARS USED FOR ASTRONOMY

Star	α(1950.0)	δ(1950.0)
1.....	03 34 59.71	−05 13 04.0
2.....	03 35 02.64	−05 12 05.9
3.....	03 35 16.93	−05 13 19.7
4.....	03 35 19.23	−05 11 57.7
5.....	03 35 21.42	−05 10 29.8
6.....	03 35 26.86	−05 10 50.6

NOTE.—Units of right ascension are hours, minutes, and seconds, and units of declination are degrees, arcminutes, and arcseconds.

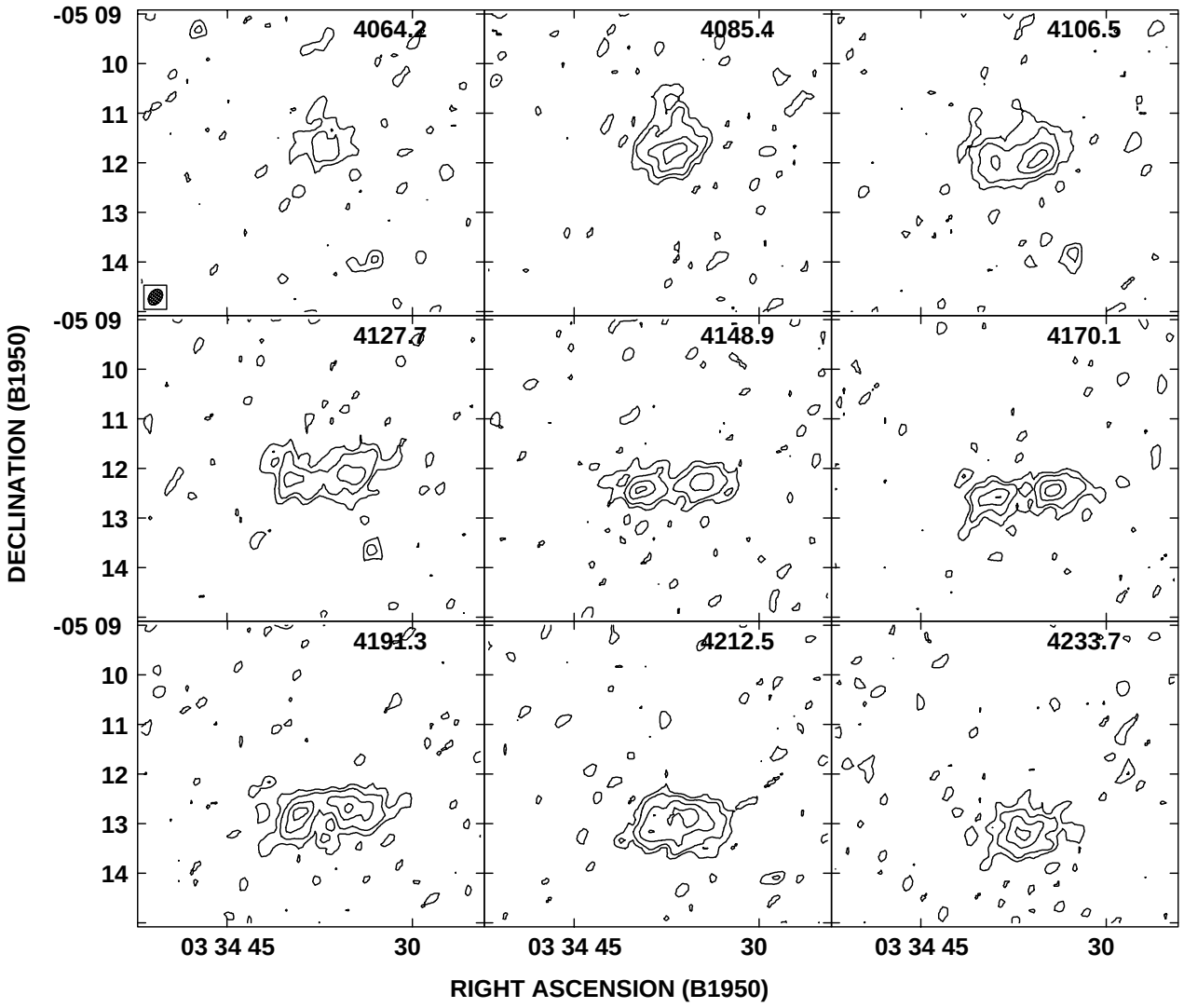

FIG. 2.—Same as Figure 1, but for the H I distribution of the bright spiral galaxy NGC 1376. Contours represent 1 (2 σ), 2, 4, 6, and 8 mJy beam^{-1}.

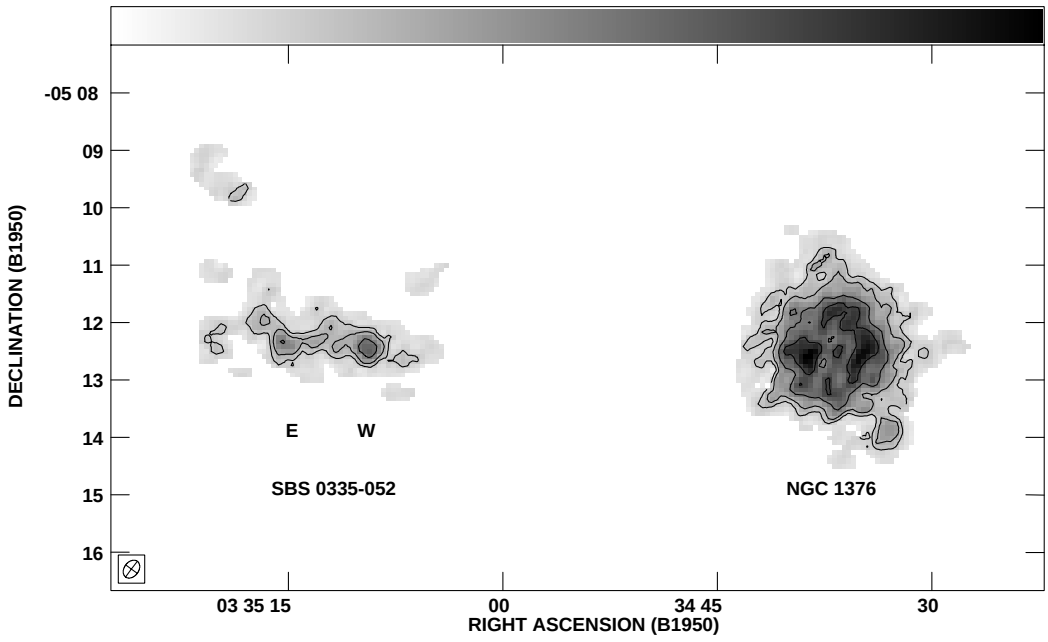

FIG. 3.—Total H I map of SBS 0335−052 and companion galaxy NGC 1376, based on the low velocity resolution data. Contours represent [1.9 (5 σ), 3.8, 7.6, and 11.4] $\times$ 10^{20} cm^{-2}. The gray scale is a linear representation of H I surface density ranging from 0 (*white*) to 16 $\times$ 10^{20} cm^{-2}. The ellipse in the lower left corner indicates the beam size.

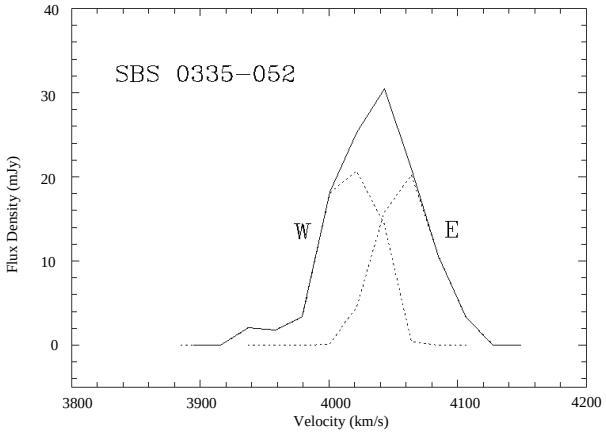

FIG. 4.—Integrated profile of H I flux (in millijanskys) for the entire H I cloud (*solid line*) in the system SBS 0335−052, as derived from the channel maps displayed in Fig. 1 for the low velocity resolution data. The total flux integrated over this profile is 2.46 Jy km s^{-1}. Dashed profiles show separate integrated profiles for the east and west components.

with superposed isovelocity lines with a contour interval of 5 km s^{-1}. The velocity field of the H I gas is quite complex. There is a general gradient across the system from 4065 km s^{-1} at the eastern edge to 4000 km s^{-1} on the western rim. However, there are clear deviations from this trend near the eastern and western peaks. This is perhaps better illustrated in Figure 7, a position-velocity (P-V) diagram made along a line through the two peaks and based on the low velocity resolution data. If the H I complex is treated as a single system, then there is a velocity gradient across it, with a maximum velocity difference of $\sim$80 km s^{-1} between the two sides. If it is considered, however, as two distinct H I clouds, then the velocity gradients are solid-body in nature, with maximum velocity differences of $\sim$35–40 km s^{-1} within each cloud.

4. RESULTS

As mentioned in the previous section, we derive an integrated H I flux of 2.46 Jy km s^{-1} over the area occupied by the cloud. This corresponds to a total H I mass of $M_{\rm H\,I} = 1.68 \times 10^9\ M_\odot$. Since the blue luminosities of the eastern and western galaxies are 7.3×10^8 and $0.82 \times 10^8\ L_\odot$, respectively, the $M_{\rm H\,I}/L_{\rm B}$ of the SBS 0335−052 system is of order 2.1.

Accounting for a mass fraction of 0.245 for helium (Izotov & Thuan 1998), the total gas mass in the system is

$$M_{\rm gas} = 2.1 \times 10^9 M_\odot\ . \quad (1)$$

With a Salpeter initial mass function, with lower and upper mass limits of 0.8 and 120 $M_\odot$, respectively, and by using the models of Schaerer & Vacca (1998), Papaderos et al. (1998) have derived a total stellar mass for the starburst and underlying stellar components of $3.1 \times 10^6\ M_\odot$. Reducing the lower mass limit to 0.1 $M_\odot$ would increase the total stellar mass to $\approx 3.7 \times 10^7\ M_\odot$. From midinfrared observations, Thuan, Sauvage, & Madden (1999b) have found that as much as three-quarters of the current star formation activity in SBS 0335−052 can be hidden by dust. Correcting for this effect would bring the total stellar mass to 7.3×10^6 and $8.8 \times 10^7\ M_\odot$ for lower mass cutoffs of 0.8 and 0.1 $M_\odot$, respectively.

Since SBS 0335−052W is about 1 order of magnitude less luminous and slightly less chemically evolved, its stellar

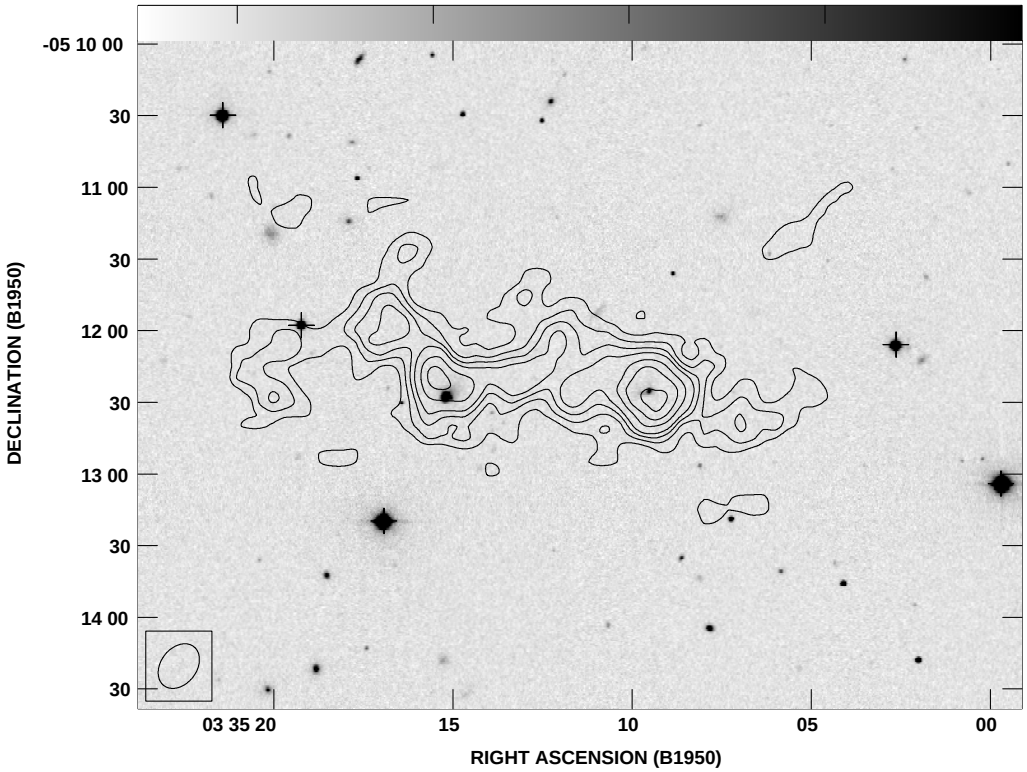

FIG. 5.—Overlay of the H I contours on an optical *B*-band image from Papaderos et al. (1998). The crosses mark the bright stars in the frame that have been used to adjust the overlay. The brightness levels of the *B* image are presented on a linear scale and in arbitrary units. H I contours represent [0.75 (2 σ), 1.8, 2.7, 3.6, 5.4, 7.2, and 9.0] $\times$ 10^{20} cm^{-2}.

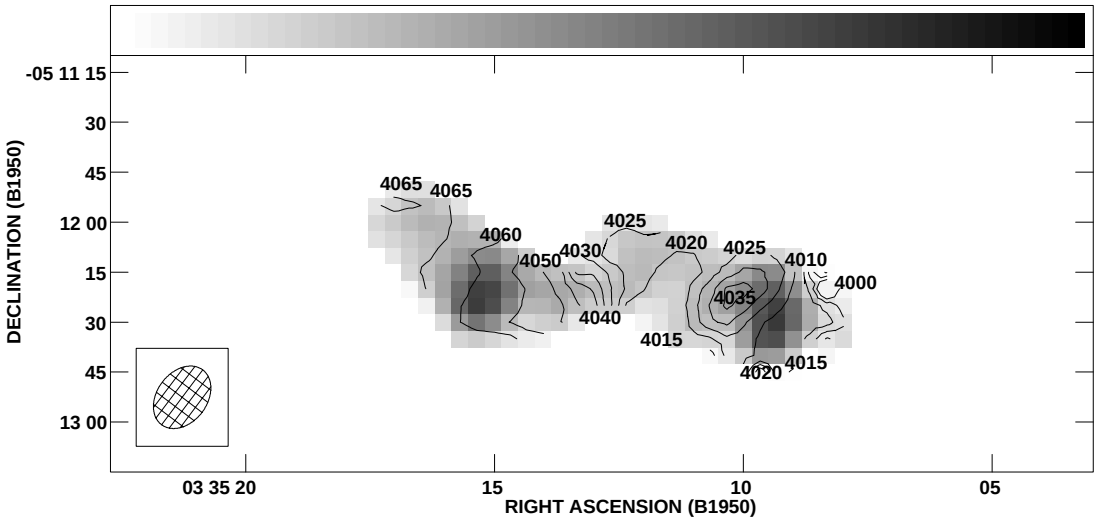

FIG. 6.—Isovelocity lines of H I superposed on the H I surface brightness map. The gray scale is a linear representation of H I surface density ranging from 0 (*white*) to 11×10^{20} cm^{-2}.

mass is expected to be about 10 times lower than that of the eastern galaxy. Thus the total stellar mass in both dwarf galaxies is at most $10^8\ M_\odot$, or no more than 5% of the total gas mass.

The two peaks in the distribution of the integrated H I map are partly resolved with the synthesized beam of 20.″5 × 15.″0 (or 5.4 × 3.9 kpc at the adopted distance of 54.3 Mpc). The position angle of the beam is P.A. = −37°. We used the AIPS task IMFIT to estimate the properties of both H I peaks. The central brightness of the western peak is 25.8 K km s^{-1}, and its FWHM size after deconvolution with the beam is (26.″7 ± 1.″5) × (15.″6 ± 1.″5) at P.A. = 53° ± 7°. For the eastern peak we get a central brightness of 19.2 K km s^{-1} and a FWHM size after deconvolution of (28.″4 ± 1.″7) × (12.″7 ± 4.″9) at P.A. = 53° ± 9°. These central brightnesses correspond to column densities of

$$N_{\mathrm{H\,I,west}} = 10.0 \times 10^{20}\ \mathrm{cm}^{-2} = 8.0\ M_\odot\ \mathrm{pc}^{-2}\ , \quad (2)$$

$$N_{\mathrm{H\,I,east}} = 7.4 \times 10^{20}\ \mathrm{cm}^{-2} = 6.0\ M_\odot\ \mathrm{pc}^{-2}\ . \quad (3)$$

The faintest regions of the outer H I disk (roughly corresponding to a 2 σ noise level over two consecutive channels) correspond to column densities of 7.5×10^{19} cm^{-2}, or about 0.6 $M_\odot$ pc^{-2}. Both H I concentrations are elongated and oriented at the same position angle, roughly southwest to northeast. Their FWHM angular sizes are very similar and correspond to a linear extent of about 7.1 × 3.7 kpc. In the southwest-northeast direction the intrinsic (deconvolved) width of both H I peaks is about a factor of 2 larger than that of the VLA beam, but in the perpendicular direction it is only 0.7–0.8 of the beam width.

The masses of the eastern and western components, by simply dividing the entire cloud in two halves as was done in Figure 4, lead to gas masses (corrected for He) of

$$M_{\mathrm{gas,west}} = 1.11 \times 10^9\ M_\odot\ , \quad (4)$$

$$M_{\mathrm{gas,east}} = 0.99 \times 10^9\ M_\odot\ .$$

The peak column density, measured for the eastern peak, 7.4×10^{20} cm^{-2}, is a factor of 10 lower than the value derived from Lyα absorption based on *HST* observations (Thuan & Izotov 1997). This is also a factor of 4 less than the peak brightness of H I for I Zw 18, as derived from VLA observations by van Zee et al. (1998b) with a synthesized beam of ∼5″ (corresponding to a linear resolution of 0.25 kpc). Both facts seem to indicate that despite the fact that some fraction of the brightest parts of the SBS 0335−052 H I complex is resolved by our VLA beam, structure at scales significantly smaller than the beam must exist and the structure of the neutral gas in the vicinity of the region with high current SF rate is clumpy, explaining the difference in

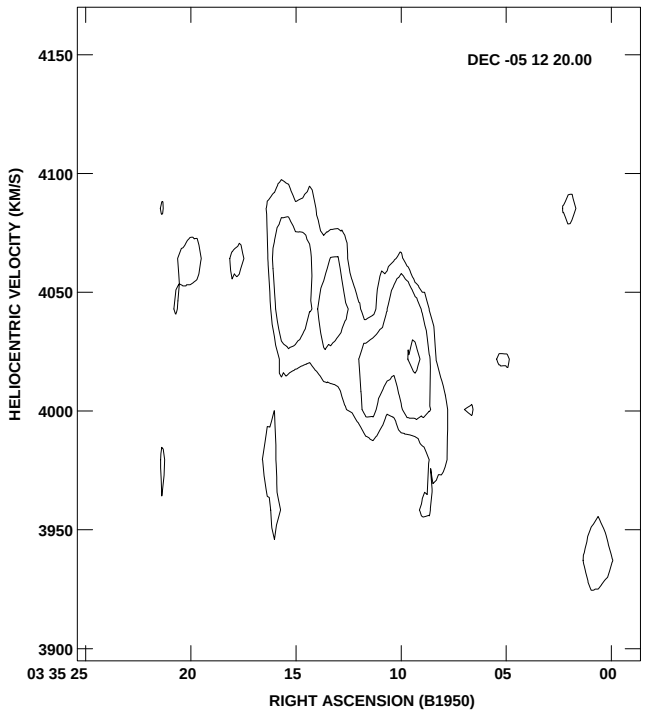

FIG. 7.—Position-velocity slice through the H I emission associated with SBS 0335−052 along an east-west line, cutting through both the eastern and western H I emission peaks. Contours represent 1.0 (2 σ), 2, 4, and 6 mJy beam^{-1}. The declination along which the slice was taken is given in the top right corner.

the peak H I column density derived from fitting the damped Lyα line profile (Thuan & Izotov 1997) and that derived here. Probably an inhomogeneous gas distribution due to H II regions and supernova remnant shells affects the structure of the neutral interstellar medium. Such shell structure is already hinted at by the optical image obtained by Melnick et al. (1992) and confirmed on *HST* images by Thuan et al. (1997).

The coordinates of the H I peaks, determined with the AIPS task IMFIT, as defined by the centers of Gaussian components, are presented in Table 3. Their rms uncertainties are $0^s.18 \times 1''.3$ for the eastern H I peak and $0^s.11 \times 0''.8$ for the western one.

The optical position of SBS 0335−052W coincides within the errors with the position of the corresponding H I peak. For SBS 0335−052, while there is no shift in right ascension between the optical and H I peaks within the cited errors, there exists a difference in declination, $\Delta\delta = +6''.1$. This is more than twice the combined error in declination and seems significant. To check the reality of this offset, we have also compared the optical image with a map made with only the C configuration data. The displacement is still present. Taken at face value, the shift between the optical and H I peaks for SBS 0335−052 is about 1.6 kpc, which corresponds to the offsets reported by, e.g., Viallefond & Thuan (1983). Note, however that van Zee et al. (1998a, 1998b), using higher spatial resolution H I maps, find no significant offset between the peaks of the H I and optical intensity distributions in the BCD I Zw 18.

Spectroscopy of the newly discovered galaxy at the position of the western peak with the 6 m telescope (Pustilnik et al. 1997) and with the Multiple Mirror and Keck II telescopes (Lipovetsky et al. 1999) reveals an emission-line spectrum with a radial velocity close to that of the H I cloud. SBS 0335−052W, with an absolute magnitude, M_B, about −14.3, like SBS 0335−052, is an extremely metal-deficient object. Its metallicity is 1/50 that of the Sun, comparable to that of I Zw 18.

The total dynamical mass is difficult to determine as this depends crucially on one's interpretation of the SBS 0335−052 system. In this paper we will present two strawman hypotheses. The first one is based on the assumption that the system is in fact one cloud with two condensations. The second hypothesis is that we are witnessing the interaction of two systems and that the observed H I shows a tidal bridge between both optical galaxies and tidal tails stretching toward the northeast and west.

For the case of one giant cloud, we can estimate the total gravitational mass by equating the centrifugal and gravitational forces at the edges of the disk. We take for the maximum rotational velocity 40 km s^{-1}, and for a radius of the disk, 16 kpc (Fig. 7). The resulting estimated lower limit for the total dynamical mass is

$$M_{\rm dyn}(R < 16\ {\rm kpc}) = 5.9 \times 10^9\ M_\odot\ . \qquad (5)$$

For the case of two interacting clouds we estimate, based on the position-velocity diagram (Fig. 7), a full width to zero velocity range of 65 km s^{-1} for SBS 0335−052 and 75 km s^{-1} for SBS 0335−052W. The linear sizes of the H I clouds are at most 12 kpc (using the full extent rather than the FWHM along the major axis of each object). We then find

$$M_{\rm dyn,\,east} = 1.6 \times 10^9\ M_\odot\ ,$$
$$M_{\rm dyn,\,west} = 2.2 \times 10^9\ M_\odot\ , \qquad (6)$$

or a total mass (east + west) of $M_{\rm dyn} = 3.8 \times 10^9\ M_\odot$, 64% of that derived on the basis of the more extreme hypothesis, that of the objects forming one cloud. It should be noted that these estimates are strict *lower* limits, as the inclination is completely unknown and was assumed to be 90° (or edge-on).

TABLE 3

SOME OBSERVED AND DERIVED CHARACTERISTICS OF THE SBS 0335−052 SYSTEM

Parameter	0335–052W	0335–052E	References
α(1950.0) (optical)[a]	03 35 09.53	03 35 15.17	4
δ(1950.0) (optical)[a]	−05 12 25.2	−05 12 27.6	4
B (mag)	19.37	17.00	1
L_B ($10^8\ L_{B\odot}$)[d]	0.82	7.3	1
Optical angular size (arcsec)[b]	14 × 14	23 × 20	1
Optical linear size (kpc)	3.7 × 3.7	6 × 5.3	1
$V_{\rm opt}$ (km s^{-1})	4069 ± 20	4060 ± 12	2, 3
$V_{\rm H\,I}$ (km s^{-1})	4017 ± 5	4057 ± 5	4
α(1950.0) (H I)	03 35 09.50	03 35 15.21	4
δ(1950.0) (H I)	−05 12 25.5	−05 12 21.5	4
Peak $N_{\rm H\,I}$ (10^{20} cm^{-2})	9.98	7.42	4
Peak H I mass surface density ($M_\odot$ pc^{-2})	8.0	6.0	4
M_B^0	−14.3	−16.7	1
H I angular size (arcsec)[c]	128 × 67	122 × 83	4
H I linear size (kpc)	33.7 × 17.6	32.1 × 21.8	4
$M_{\rm H\,I}$ ($M_\odot/10^8$)	8.9	8.0	4
$M_{\rm H\,I}/L_B$ ($M_\odot/L_{B\odot}$)	10.8	1.1	4
$M_{\rm tot}/L_B$ ($M_\odot/L_{B\odot}$)	26.8	2.2	4

[a] Optical coordinates derived from DSS images.
[b] Optical size corresponding to the isophotal level of 27.5 mag arcsec^{-2} in B (Papaderos et al. 1998).
[c] Maximum observed extent of the associated H I gas.
[d] $L_{B\odot}$ is the solar blue luminosity corresponding to $M_{B\odot} = 5.48$.

REFERENCES.— (1) Papaderos et al. 1998; (2) Lipovetsky et al. 1999; (3) Izotov et al. 1997; (4) This paper.

We have shown that in both hypotheses we need to invoke substantial amounts of dark matter to reconcile the observed baryonic content with the dynamical masses derived on the basis of the observed kinematics. To obtain yet another (lower) limit to the amount of dark matter that might be hiding within the SBS 0335−052 system, we can take the observed (projected) separation and radial velocity difference and calculate the mass that this implies assuming the two clouds are in a bound orbit. This works out to be $M_{\rm tot} = 9 \times 10^9\ M_\odot$ (see van Moorsel 1987 for details). Therefore, both the individual clouds, as well as the SBS 0335−052 system, require substantial amounts of nonvisible matter to make up for the inferred masses, based on their dynamics.

5. DISCUSSION

5.1. *SBS 0335−052 in Relation to Other Candidate Young Galaxies*

It is interesting to compare this system with other candidate young galaxies. There are three galaxies in the literature with similar characteristics that have been proposed as possible young objects: I Zw 18, ESO 400-G43, and H I 1225+01.

The H I in I Zw 18 has a complex structure with three distinct H I components (Viallefond et al. 1987; van Zee et al. 1998b), two of them associated with star-forming regions: the northwestern and southeastern components in the main body of the galaxy and component C to the north (e.g., Dufour et al. 1996). But unlike SBS 0335−052, in which the two centers of star formation are well separated spatially, the three star-forming regions in I Zw 18 are connected causally, with star formation self-propagating from component C to the southeastern component (Izotov & Thuan 1998).

In ESO 400-G43 (Bergvall & Jörsäter 1988), the two H I components are well separated by a projected distance of ∼40 kpc, each component containing an optical counterpart. Only one of the optical galaxies has been studied in detail. It has been described as a possible young galaxy, although its metallicity, $Z = Z_\odot/8$, is probably too high for it to be forming its first generation of stars (see Izotov & Thuan 1999).

The H I 1225+01 system (Salzer et al. 1991; Chengalur et al. 1995), at a distance of 20 Mpc, presents several similarities to the H I envelope associated with SBS 0335−052. It also has two extended components, separated by a projected distance of 98 kpc with an H I tidal bridge linking them. A dwarf H II galaxy 12 kpc in size is located within the 40 kpc northeastern H I component, approximately at the position of the H I peak. The total gas mass of the northeastern H I component, $\sim 3 \times 10^9\ M_\odot$, is close to that of the H I gas in the SBS 0335−052 system. The dynamical mass is a factor of 3 larger than the gas mass. Because of a smaller inclination angle ($i \sim 30°$) and better spatial and velocity resolution, the authors are able to distinguish barlike and spiral structure in the northeastern H I component.

The very low metallicity, $Z \sim 1/20\ Z_\odot$, in the H II region associated with the current SF burst and the very low mass fraction in the form of stars suggest that the H I 1225+01 system probably is in the process of forming its first generation of stars. One of the arguments of Salzer et al. (1991), who claim that the current SF burst in this H II galaxy is possibly not the first one, is that there is a significant abundance of nitrogen, which the authors assume to be produced by intermediate-mass stars. However, as mentioned earlier, the finding of a constant N/O ratio with a very small dispersion in the most metal-poor BCDs, those with $Z < Z_\odot/20$ (Thuan et al. 1995; Izotov & Thuan 1999), strongly suggests primary production of nitrogen by massive stars in galaxies as metal-deficient as SBS 0335−052, and thus there is no need for a second burst of star formation in the optical counterpart of H I 1225+01 to account for the nitrogen abundance. The second H I component has no detectable optical emission but shows a velocity field corresponding to that of an inclined rotating disk. Thus Chengalur et al. (1995) suggest that the most probable interpretation for this system is as an SF burst in a primordial H I cloud (the northeastern component) due to the tidal action of another massive H I cloud.

The H I properties of the SBS 0335−052 system also show some similarities with those of II Zw 40 (Brinks & Klein 1988; van Zee et al. 1998a). The metallicity of this BCD is $\sim Z_\odot/6$, considerably higher than those of the systems mentioned above and suggesting that this galaxy is more evolved than SBS 0335−052 and not necessarily its analog. Nevertheless it is instructive to compare the two objects briefly to discuss their different evolutionary states. The II Zw 40 system is most likely a merger, showing two H I tidal tails of ∼6.5 and 15 kpc in size. The extent of the H I gas and the H I masses of the tails are reminiscent of the situation in SBS 0335−052. However, the optical morphologies of SBS 0335−052 and II Zw 40 differ. Whereas II Zw 40 resembles an advanced merger with optical tidal tails (van Zee et al. 1998a), SBS 0335−052 exhibits two regular-looking, still widely separated dwarf galaxies that are perhaps in an earlier stage of what could evolve into a merger. Over time, SBS 0335−052 might very well develop into a system resembling II Zw 40.

5.2. *Possible Star Formation Triggers*

One of the unsolved problems ever since the discovery of the first BCDs (Sargent & Searle 1970) concerns the triggering mechanism for the star formation. And perhaps even more baffling, Why has star formation not occurred earlier in the lifetime of these objects?

In all likelihood, tidal triggering is probably responsible for the current star formation in the SBS 0335−052 system. We shall again consider two hypotheses: (1) the case in which SBS 0335−052 is one huge H I cloud containing two star-forming centers and (2) the case in which the BCDs are the nuclei of two distinct interacting H I clouds.

In the case of a single self-gravitating H I cloud, the tidal triggering is probably due to the companion massive galaxy NGC 1376, whose H I map is shown in Figure 8. The resolution of the map is too low to say much about the H I morphology. However, we can note that the H I gas, as usual, is more extended than the optical disk and that there is a conspicuous lack of H I in the nuclear region of the galaxy. A lower limit to the distance between the galaxy and the SBS 0335−052 system is their observed projected distance of 150 kpc. NGC 1376 is an Scd galaxy with $m_{\rm pg} = 12.8$, $M_B = -21.0$, optical diameter $D = 2\farcm0$, and inclination 21°. Its H I profile is characterized by a full width at 20% of peak intensity of 179 km s^{-1} and a heliocentric radial velocity $V_{\rm H\,I} = 4162$ km s^{-1}. It is a member of a medium-density group listed as LGG 103 (Garcia 1993) and

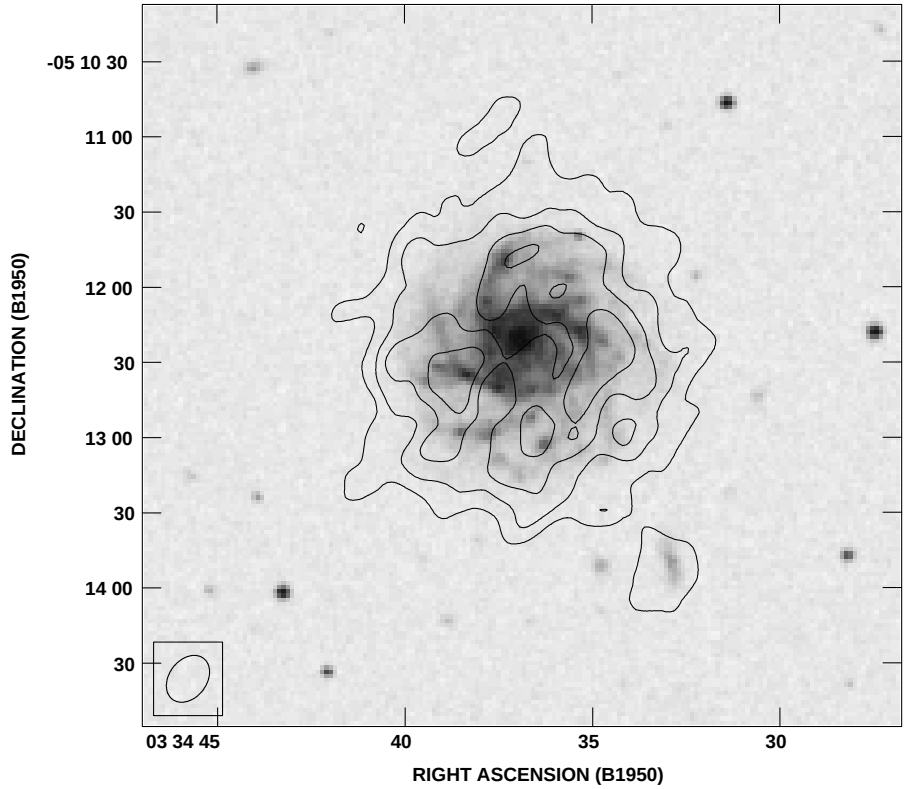

FIG. 8.—Overlay of the H I contours on a DSS image of NGC 1376. Contour levels are at [3.8, 7.6, 11.4, and 15.2] $\times 10^{20}$ cm^{-2}. There is a small H I blob southwest of NGC 1376, which coincides with a low surface brightness dwarf galaxy not listed in NED.

composed of at least 14 galaxies. NGC 1376 is situated on its southwestern outskirts. The closest known group member is at a projected distance of about 0.7 Mpc. Rix & Zaritzky (1995) note that NGC 1376 has three spiral arms, and Elmegreen & Elmegreen (1987) assign this galaxy to class 2 in their classification of spiral galaxies, which means that its arms are "fragmented spiral pieces with no regular pattern." This suggests that the spiral has recently experienced a tidal disturbance.

The VLA H I data do point to a small galaxy, a companion to NGC 1376, that may be at the origin of that tidal disturbance. Figure 8 shows a small irregular H I blob southwest of the main body of NGC 1376 at $(\alpha, \delta) = (03^h34^m32^s.9, -05°13'51'')$. Its detection is weak but fairly reliable as it can be seen in at least two neighboring channel maps at heliocentric velocity 4117 ± 5 km s^{-1}. Its integrated flux density is 0.17 Jy km s^{-1}, which corresponds to an H I mass of $1.2 \times 10^8\ M_\odot$ at the distance 54.3 Mpc. This blob is kinematically detached from the regular velocity field of the galaxy and can be identified optically on the Deep Sky Survey (DSS) with what appears to be a faint elongated dwarf companion not listed in the NASA/IPAC Extragalactic Database (NED), with diameter $\sim 23''$ (i.e., linear size ~ 6 kpc) at projected distance 27.5 kpc from NGC 1376. The H I profile of the dwarf galaxy is two channels wide so that its velocity width is ~ 42 km s^{-1}. This yields a lower limit (the inclination being unknown) of $\sim 2.5 \times 10^8\ M_\odot$ for its dynamical mass.

The total dynamical mass of NGC 1376 as estimated from the width of the H I profile (inclination corrected to $V_{\rm rot} = 250$ km s^{-1}) and the radius of the H I distribution is about $5 \times 10^{11}\ M_\odot$. By taking into account the results by Zaritsky & White (1994) and Zaritsky et al. (1997) on distant dwarf satellites of spiral galaxies and masses of their dark matter halos, the total gravitational mass of NGC 1376 exerting a tidal force on SBS 0335−052 can be up to twice that value, or $10^{12}\ M_\odot$. A detailed understanding of the triggering mechanism of an SF burst due to tidal forcing such as that due to NGC 1376 is still lacking. It will require a more careful study and modeling that is beyond the scope of this paper. However, it is clear from some simple estimates that this massive spiral galaxy is close enough to the H I complex to induce in it a gravitational instability via mechanisms such as those suggested by Icke (1985), Noguchi (1988), and Olson & Kwan (1990a, 1990b). The mechanism proposed by Noguchi (1988) generates a central bar, which in turn causes gas to sink toward the center of the disk and induce its collapse. No observational evidence is seen, neither for a central barlike structure in the H I cloud of SBS 0335−052 nor for a central density concentration. The mechanism proposed by Olson & Kwan (1990a, 1990b) works via a large tidal increase of the inelastic collision rate of individual gas clouds and their merging and collapse. It is basically a stochastic process.

The most probable mechanism is that proposed by Icke (1985) involving tidal acceleration to supersonic velocities of gas layers in the external parts of an H I disk, with subsequent dissipation of the kinetic energy and loss of dynamical stability of the gas disk. It requires only a moderate tidal force and acts from larger distances in comparison with the two other mechanisms.

Adopting a radius $R = 16$ kpc for the H I disk, a circular velocity V of 40 km s^{-1} at R, a dynamical mass within R of $6 \times 10^9\ M_\odot$ for the SBS 0335−052 system, a total dynamical mass of $10^{12}\ M_\odot$ for NGC 1376, and a sound speed of the H I gas of 10 km s^{-1}, we find that for pericenter dis-

tances smaller than ∼412 kpc, the gas in SBS 0335−052 can be accelerated to supersonic velocities. This distance is significantly larger than the present projected distance of 150 kpc so that sufficiently strong tidal forces of NGC 1376 on the H I complex are expected. Such a tidal triggering mechanism may explain the fact that the two star-forming centers began nearly simultaneously and are aligned along the line joining the centers of the two objects, symmetrically on each side of the center of the SBS 0335−052 system, just as the tidal forces of the moon on Earth cause high ocean tides on diametrically opposite locations on Earth.

Alternatively, we may consider that we do not have a single huge H I complex but two distinct smaller H I components interacting tidally with each other and triggering star formation at the location of the two H I peaks. In this case, the tidal force F_1 exerted by each cloud is proportional to $M(\text{cloud})/d_1^3$, where d_1 is the projected separation between the two BCDs. On the other hand, the tidal force F_2 exerted by NGC 1376 is proportional to $M(\text{NGC 1376})/d_2^3$, where d_2 is the projected separation between the galaxy and the SBS 0335−052 system. By adopting $M(\text{cloud}) = 2 \times 10^9\ M_\odot$, $M\ (\text{NGC 1376}) = 10^{12}\ M_\odot$, $d_1 =$ 22 kpc, and $d_2 = 150$ kpc, we find $F_1/F_2 = 0.6$, i.e., the tidal forces in the two cases are comparable and we cannot say for sure which of the two scenarios discussed above prevails. In the case of two distinct H I components, we find that the Icke (1985) mechanism applies to pericenter distances less than ∼27 kpc.

Clearly, detailed hydrodynamical calculations of the tidal interaction between two H I clouds and between a massive galaxy such as NGC 1376 and a primordial gas cloud similar to that associated with SBS 0335−052 are needed to understand better the triggering of star formation in these systems.

5.3. *Star Formation Threshold*

Star formation in disk galaxies is thought to occur above a critical threshold of the gas surface density above which clouds will become gravitationally unstable against collapse (Toomre 1964; Kennicutt 1989). This critical density is proportional to the velocity dispersion of the gas disk and the epicyclic frequency, which is twice the circular frequency for regions with solid-body rotation. The validity of the Kennicutt (1989) H I column density threshold for onset of star formation has been checked for BCDs (e.g., Taylor et al. 1994), as well as for LSB galaxies (van der Hulst et al. 1993). Alternatively, as first mentioned by Skillman (1987), star formation in dwarf irregulars occurs when the column densities reach values of order $5 \times 10^{20}\ \text{cm}^{-2}$; this threshold increases with decreasing metallicity (Franco & Cox 1986).

The observed peak column densities in the SBS 0335−052 system coinciding with the optical counterparts are near the upper end of the range of those reported for H II galaxies by Taylor et al. (1993, 1995), namely, $(0.8\text{–}11) \times 10^{20}\ \text{cm}^{-2}$, when compared with data on objects mapped with comparable linear resolution of order 5 kpc. These values are also in the same range, $(1.0\text{–}10.5) \times 10^{20}\ \text{cm}^{-2}$, observed for LSB galaxies, objects in which no significant star formation takes place, and observed by van der Hulst et al. (1993) with a similar linear resolution.

Given our modest spatial resolution, all we can do is make an order-of-magnitude estimate of the expected threshold value and compare that with the observed (beam smeared) ones. To obtain an estimate we assume that both peaks fall within the solid-body part of the rotation curve, at a rotational velocity of about 20 km s^{-1} and a radial distance of 6 kpc. With a typical gas velocity dispersion σ_v of 6 km s^{-1}, we obtain for the critical surface density at the radius of the current SF burst a value equal to only 1.3 $M_\odot$ pc^{-2} (eq. [6] of Kennicutt 1989 with $\alpha = \frac{2}{3}$), in comparison with the measured values 8.0 and 6.0 $M_\odot$ pc^{-2}. With a viewing angle of the H I disk of less than 77°, the gravitational instability condition would be satisfied. This appears to be the case since in the simple model of a circular flattened H I disk, the observed axial ratio would correspond to a viewing angle of 70°.

5.4. *Role of a Dark Matter Halo*

It has been shown (e.g., de Blok, McGaugh, & van der Hulst 1996) that LSB galaxies are dominated by dark matter over the entire area where H I and stellar emission is detected. This dark matter dominance is one of the main factors that allows an LSB galaxy to be stable against various perturbations (see, e.g., the study of the relative fragility of LSB and high surface brightness disks by Mihos, McGaugh, & de Blok 1997). If in the SBS 0335−052 system we indeed observe the formation of a first generation of stars in a low-density primordial gas cloud, then its dark matter halo should have played an especially important role for stabilizing the gas against various local and global instabilities and preventing it from gravitationally collapsing and forming stars. Presumably a strong tidal perturbation due to either a close passage of a massive galaxy or the interaction with another H I cloud can overcome the stabilizing influence of the dark matter halo and trigger a starburst.

6. CONCLUSIONS

From the observational data presented here and the properties derived for the H I gas and based on the discussion above we arrive at the following conclusions:

1. The optical dwarf galaxy SBS 0335−052 is associated with a huge H I cloud of overall size 66 × 22 kpc, elongated in the east-west direction. The cloud has a total H I mass of $1.68 \times 10^9\ M_\odot$.

2. This H I cloud contains two prominent H I peaks, located nearly symmetrically to the east and west, and separated by about 22 kpc. They measure 7 × 4 kpc and contain 0.79×10^9 and $0.89 \times 10^9\ M_\odot$, respectively, of H I.

3. The two H I density peaks are identified with two optical emission-line dwarf galaxies, the eastern one with SBS 0335−052 itself and the western one with a new, less luminous (by 1 order of magnitude) dwarf named SBS 0335−052W. This latter galaxy shows very similar properties, including an extremely low metallicity of the H II region gas, consistent with the amount produced during a first SF burst. Radial velocities of these galaxies, as measured from the emission lines of their H II regions, are very close to those of the H I gas at the positions of their respective peaks.

4. The velocity field of the H I cloud is rather disturbed, with presumably tidal tails protruding from both edges of the cloud. This suggests that what we are seeing is an interaction, possibly with the nearby galaxy NGC 1376. This large spiral galaxy, the dominant member of the galaxy group LGG 103, with a radial velocity of 120 km s^{-1} larger than that of SBS 0335−052, is located at a projected distance of 150 kpc. Consideration of the relevant parameters

of the SBS 0335−052 system and NGC 1376 does not contradict the hypothesis that the formation of the two young dwarfs from the huge low surface density H I cloud was triggered by a tidal interaction with NGC 1376.

5. Alternatively, we are dealing with two almost equal-mass H I clouds, each measuring $\sim 7 \times 4$ kpc, each containing an optical counterpart, and each showing solid-body rotation with an amplitude of $\sim$35–40 km s^{-1}. In this case, the triggering of the star formation in the two H I clouds is probably due to their mutual tidal interaction.

6. Each component seems to require the presence of dark matter, and the system as a whole is dominated by a dark matter halo. The total dynamical mass of the system is estimated to be between 3.8×10^9 and 9×10^9 $M_\odot$, or $\sim$1.9 to 4.5 times larger than the total mass of gas and stars.

7. If the viewing angle of the H I disk is less than 77°, the gas surface densities for both H I peaks are larger than the critical value determined from the parameters of the rotation curve at those radii and are consistent with the onset of gravitational instability and subsequent star formation.

We thank the partial financial support of NATO collaborative research grant 921285 (S. A. P. and T. X. T.), INTAS grant 94-2285 (S. A. P. and Y. I. I.), NSF grant AST 96-16863 (T. X. T. and Y. I. I.), Russian grant RFBR 97-02-16755 (S. A. P.) and CONACyT grant 0460P-E (E. B.). S. A. P. is grateful to the NRAO staff at Socorro for hospitality and support with the VLA data reduction and to Oleg Verkhodanov and Pat Murphy for help with installing AIPS at the Special Astrophysical Observatory. The *B* optical image of the SBS 0335−052 system was kindly provided by Polychronis Papaderos. The anonymous referee made useful suggestions, which helped to improve the presentation of the paper. We have used the NASA/IPAC Extragalactic Database (NED), operated by the Jet Propulsion Laboratory, California Institute of Technology, under contract with the National Aeronautics and Space Administration. We have also used the Digitized Sky Survey, produced at the Space Telescope Science Institute under government grant NAG W-2166.

REFERENCES

Bergvall, N., & Jörsäter, S. 1988, Nature, 331, 589
Brinks, E., & Klein, U. 1988, MNRAS, 231, P63
Chengalur, J. N., Giovanelli, R., & Haynes, M. P. 1995, AJ, 109, 2415
de Blok, W. J. G., McGaugh, S. S., & van der Hulst, J. M. 1996, MNRAS, 283, 18
Dey, A., Spinrad, H., Stern, D., Graham, J. R., & Chaffee, F. H. 1998, ApJ, 498, L93
Dufour, R. J., Garnett, D. R., Skillman, E. D., & Shields, G. A. 1996, in ASP Conf. Ser. 98, From Stars to Galaxies, ed. C. Leitherer, U. Fritze-von Alvensleben, & J. Huchra (San Francisco: ASP), 358
Elmegreen, D., & Elmegreen, B. 1987, ApJ, 314, 3
Franco, J., & Cox, D. P. 1986, PASP, 98, 1076
Garcia, A. M. 1993, A&AS, 100, 47
Icke, V. 1985, A&A, 144, 115
Izotov, Y. I., Chaffee, F. H., Foltz, C. B., Green, R. B., Guseva, N. G., & Thuan, T. X. 1999, ApJ, 527, 757
Izotov, Y. I., Lipovetsky, V. A., Chaffee, F. H., Foltz, C. B., Guseva, N. G., & Kniazev, A. Y. 1997, ApJ, 476, 698
Izotov, Y. I., Lipovetsky, V. A., Guseva, N. G., Kniazev, A. Y., & Stepanian, J. A. 1990, Nature, 343, 238
Izotov, Y. I., & Thuan, T. X. 1998, ApJ, 497, 227
———. 1999, ApJ, 511, 639
Kennicutt, R. C. 1989, ApJ, 344, 685
Kunth, D., Lequeux, J., Sargent, W. L. W., & Viallefond, F. 1994, A&A, 282, 709
Lasker, B. M., Sturch, C. R., McLean, B. J., Russell, J. L., Jenkner, H., & Shara, M. M. 1990, AJ, 99, 2019
Lequeux, J., Peimbert, M., Rayo, J. F., Serrano, A., & Torres-Peimbert, S. 1979, A&A, 80, 155
Lequeux, J., & Viallefond, F. 1980, A&A, 91, 269
Lipovetsky, V. A., Chaffee, F. H., Izotov, Y. I., Foltz, C. B., Kniazev, A. Y., & Hopp, U. 1999, ApJ, 519, 177
Melnick, J., Heydari-Malayeri, M., & Leisy, P. 1992, A&A, 253, 16
Mihos, J. C., McGaugh, S. S., & de Blok, W. J. G. 1997, ApJ, 477, L79
Noguchi, M. 1988, A&A, 203, 259
Olson, K. M., & Kwan, J. 1990a, ApJ, 349, 480
———. 1990b, ApJ, 361, 426
Papaderos, P., Izotov, Y. I., Fricke, K. J., Guseva, N. G., & Thuan, T. X. 1998, A&A, 338, 43
Pettini, M., & Lipman, K. 1995, A&A, 297, L63
Pustilnik, S. A., Lipovetsky, V. A., Izotov, Y. I., Brinks, E., Thuan, T. X., Kniazev, A. Y., Neizvestny, S. I., & Ugryumov, A. V. 1997, Astron. Lett., 23, 308
Rix, W., & Zaritzky, D. 1995, ApJ, 447, 82
Salzer, J. J., Di Serego Alighieri, S., Matteucci, F., Giovanelli, R., & Haynes, M. 1991, AJ, 101, 1258
Sargent, W. L. W., & Searle, L. 1970, ApJ, 162, L155
Schaerer, D., & Vacca, W. D. 1998, ApJ, 497, 618
Searle, L., & Sargent, W. L. W. 1972, ApJ, 173, 25
Skillman, E. D. 1987, in Star Formation in Galaxies, ed. C. J. L. Persson (NASA CP-2466) (Washington: GPO), 263
Steidel, C., Giavalisco, M., Pettini, M., Dickinson, M., & Adelberger, K. 1996, ApJ, 462, L17
Taylor, C. L. 1997, ApJ, 480, 524
Taylor, C. L., Brinks, E., Grashuis, R. M., & Skillman, E. D. 1995, ApJS, 99, 427
———. 1996a, ApJS, 102, 189
Taylor, C. L., Brinks, E., Pogge, R. W., & Skillman, E. D. 1994, AJ, 107, 971
Taylor, C. L., Brinks, E., & Skillman, E. D. 1993, AJ, 105, 128
Taylor, C. L., Thomas, D. L., Brinks, E., & Skillman, E. D. 1996b, ApJS, 107, 143
Thuan, T. X., & Izotov, Y. I. 1997, ApJ, 489, 623
Thuan, T. X., Izotov, Y. I., & Lipovetsky, V. A. 1995, ApJ, 445, 108
———. 1997, ApJ, 477, 661
Thuan, T. X., Lipovetsky, V. A., Martin, J.-M., & Pustilnik, S. A. 1999a, A&AS, 139, 1
Thuan, T. X., & Martin, G. M. 1981, ApJ, 247, 823
Thuan, T. X., Sauvage, M., & Madden, S. 1999b, ApJ, 516, 783
Toomre, A. 1964, ApJ, 139, 1217
van der Hulst, J. M., Skillman, E. D., Smith, T. R., Bothun, G. D., McGaugh, S. S., & de Blok, W. J. G. 1993, AJ, 106, 548
van Moorsel, G. A. 1987, A&A, 176, 13
van Zee, L., Skillman, E. D., & Salzer, J. J. 1998a, AJ, 116, 1186
van Zee, L., Westpfahl, D., Haynes, M., & Salzer, J. J. 1998b, AJ, 115, 1000
Vanzi, L., Hunt, L. K., Thuan, T. X., & Izotov, Y. I. 2000, A&A, 363, 493
Viallefond, F., Lequeux, J., & Comte, G. 1987, in Starburst and Galaxy Evolution, ed. T. X. Thuan, T. Montmerle, & J. T. T. Van (Paris: Ed. Frontières), 139
Viallefond, F., & Thuan, T. X. 1983, ApJ, 269, 444
Zaritsky, D., Smith, R., Frenk, C., & White, S. D. M. 1997, ApJ, 478, 39
Zaritsky, D., & White, S. 1994, ApJ, 435, 599